

## ALMA IMAGES OF THE ORION HOT CORE AT 349 GHz

M. C. H. WRIGHT, R. L. PLAMBECK

Radio Astronomy Laboratory, University of California, Berkeley, CA 94720, USA

*submitted April 19, 2022*

### ABSTRACT

We present ALMA images of the dust and molecular line emission in the Orion Hot Core at 349 GHz. At 0.2'' angular resolution the images reveal multiple clumps in an arc  $\sim 1''$  east of Orion Source I, the protostar at the center of the Kleinmann-Low Nebula, and another chain of peaks from IRC7 towards the southwest. The molecular line images show narrow filamentary structures at velocities  $> 10 \text{ km s}^{-1}$  away from the heavily resolved ambient cloud velocity  $\sim 5 \text{ km s}^{-1}$ . Many of these filaments trace the SiO outflow from Source I, and lie along the edges of the dust emission. Molecular line emission at excitation temperatures 300–2000 K, and velocities  $> 10 \text{ km s}^{-1}$  from the ambient cloud, suggest that the Hot Core may be heated in shocks by the outflow from Source I or from the BN/SrcI explosion. The spectral line observations also reveal a remarkable molecular ring,  $\sim 2''$  south of SrcI, with a diameter  $\sim 600 \text{ AU}$ . The ring is seen in high excitation transitions of HC<sub>3</sub>N, HCN  $v_2=1$ , and SO<sub>2</sub>. An impact of ejecta from the BN/SrcI explosion with a dense dust clump could result in the observed ring of shocked material.

*Subject headings:* ISM: individual(Orion-KL) — radio continuum: stars — radio lines: stars — stars: formation — stars: individual (Hot Core)

### 1. INTRODUCTION

The Kleinmann-Low (KL) Nebula in Orion, at a distance of 415 pc (Menten et al. 2007; Kim et al. 2008), is the closest region in which high mass stars ( $M > 8 M_{\odot}$ ) are forming. The two most massive stars in the region, the Becklin-Neugebauer Object (BN) and radio Source I (hereafter, “SrcI”) appear to be recoiling from one another at  $\sim 40 \text{ km s}^{-1}$ , argued to be the result of a dynamic interaction between them 500 years ago that also launched an explosive outflow of at least  $8 M_{\odot}$  of material with velocities of 10 to  $> 100 \text{ km s}^{-1}$  (Gómez et al. 2008; Zapata et al. 2009; Goddi et al. 2011b; Bally et al. 2011, 2017). SiO emission also traces a lower velocity outflow from SrcI that extends  $\sim 1000 \text{ AU}$  into the surrounding medium along a NE-SW axis (Plambeck et al. 2009; Matthews et al. 2010; Greenhill et al. 2013), roughly perpendicular to SrcI’s proper motion.

Observations at many wavelengths, from cm to IR, reveal a dense Hot Core  $\sim 10''$  in diameter adjacent to SrcI. The Hot Core does not appear to be internally heated; no known protostars are embedded within it. Goddi et al. (2011a) mapped the Hot Core in 7 NH<sub>3</sub> lines with energy levels up to 1500 K, and suggest that it is heated by the outflow from SrcI and by the impact of SrcI’s proper motion towards it.

In this paper, we present 349 GHz, 0.2'' resolution ALMA images of the dust and molecular line emission from the Hot Core, comparing these with CARMA images of the 229 GHz dust emission and the 86 GHz SiO  $v=0$  outflow (Plambeck et al. 2013, 2009). These data suggest that both shocks from the SrcI outflow and ejecta from the BN/SrcI explosion play a role in heating the Hot Core.

### 2. OBSERVATIONS AND DATA REDUCTION

The ALMA observations at 349 GHz, made in 2014 July, were designed to image the continuum emission from SrcI, but were obtained in spectral line mode so that line free portions of the spectrum could be identified. Details of the ALMA observations are given in Plambeck & Wright (2016) Table 1. Spectral line data were obtained with  $3840 \times 0.488 \text{ MHz}$  channels in 2 polarizations in each of 4 spectral windows.

The visibility data were calibrated using ALMA-supplied scripts and the CASA software package. The calibrated CASA measurement sets then were written out in FITS format and imported into Miriad. All further processing was done with Miriad, which took about 10% of the time required by CASA.

As described in Plambeck & Wright (2016), the data were then self calibrated using continuum images generated from the line-free spectral channels. The antenna-based phase corrections were derived only from visibilities with projected baselines greater than 250 k $\lambda$  in order to avoid confusion from extended emission. These images were dominated by emission from SrcI at the center. Visibilities measured on shorter spacings sample low spatial frequency Fourier components of the source brightness distribution, primarily thermal dust emission from large scale structures like the Orion Hot Core.

### 3. CONTINUUM IMAGES

The channel-averaged visibilities for the 4 separate ALMA spectral windows were combined using multifrequency synthesis to avoid bandwidth smearing at the edge of the images. The image was deconvolved using the CLEAN algorithm. Uncertainties in the fluxes are dominated by the absolute calibration uncertainties of  $\pm 10\%$  for Band 7, as given by the ALMA Cycle 1 Technical Handbook.

We compare the ALMA 349 GHz continuum image with a CARMA 229 GHz image with similar angular resolution. The 229 GHz data were obtained in the CARMA

TABLE 1  
MOLECULAR FEATURES

| freq     | molecule              | $E_U$ |
|----------|-----------------------|-------|
| 340.7142 | SO                    | 81    |
| 340.8387 | $^{33}\text{SO}$      | 87    |
| 355.0455 | $\text{SO}_2$         | 111   |
| 355.1865 | $\text{SO}_2$         | 180   |
| 356.0406 | $\text{SO}_2$         | 230   |
| 341.2755 | $\text{SO}_2$         | 369   |
| 342.7616 | $\text{SO}_2$         | 582   |
| 341.6740 | $\text{SO}_2$         | 679   |
| 341.4031 | $\text{SO}_2$         | 808   |
| 354.8000 | $\text{SO}_2$ v2=1    | 928   |
| 342.4359 | $\text{SO}_2$ v2=1    | 1041  |
| 343.9237 | $\text{SO}_2$ v2=1    | 1058  |
| 341.3233 | $\text{SO}_2$         | 1412  |
| 341.5594 | SO v=1                | 1686  |
| 354.6975 | $\text{HC}_3\text{N}$ | 341   |
| 354.4604 | HCN v2=1              | 1067  |
| 356.2556 | HCN v2=1              | 1067  |

A- and B-configurations in 2009 and 2011. The 229 GHz calibration is described in Plambeck et al. (2013). The uv-coverage of the 229 and 349 GHz data is shown in Plambeck & Wright (2016), Figure 2.

Figure 1 displays 349 GHz and 229 GHz continuum images that were generated from the self-calibrated data using all baselines  $>40$  k $\lambda$ , with `robust=0.5` weighting.

There is good agreement between the 229 and 349 GHz emission, even though the uv-coverage is quite different between these 2 radio telescope arrays. Although our data do not fully sample the short spacings, the images at 349 and 229 GHz reveal a series of clumps of emission from the Hot Core in an arc  $\sim 1''$  east of SrcI, and another chain of peaks to the west, near the infrared source IRc7. These images are in good agreement with those presented by Hirota et al. (2015). The compact sources identified by Hirota et al. (2015) are marked by crosses in Figure 1.

Also shown in Figure 1 is the CARMA image of the 86 GHz SiO line in the ground vibrational state (Plambeck et al. 2009), which traces the bipolar outflow from SrcI. The Hot Core continuum peaks lie along the SE edge of the outflow, whilst IRc7 and several other continuum peaks trace the W boundary of the outflow.

#### 4. SPECTRAL LINES

Spectral line images were generated from the self-calibrated visibility data using all baselines  $>40$  k $\lambda$  and `robust=0.5` weighting. We made spectral line images for each of the 4 spectral windows;  $4 \times 3840$  channels in total. A multitude of molecular lines are evident in the spectra. Plambeck & Wright (2016) show the spectra at the position of SrcI, and present tables of the strongest spectral lines. Sulfur- and silicon-rich molecules such as SiO, SO,  $\text{SO}_2$ , SiS, and  $\text{H}_2\text{S}$  are particularly prominent toward SrcI. Examination of a wider field reveals a very confused picture with deep sidelobes resulting from the poorly sampled large scale structures in molecular line emission from the ambient molecular cloud. However, away from the ambient cloud velocity many of the spectral lines show narrow filamentary structures which appear to trace the dust clumps and the edges of the SiO outflow from SrcI.

We made spectral line images at  $1 \text{ km s}^{-1}$  resolution in the velocity range  $-40$  to  $+40 \text{ km s}^{-1}$  to image structures

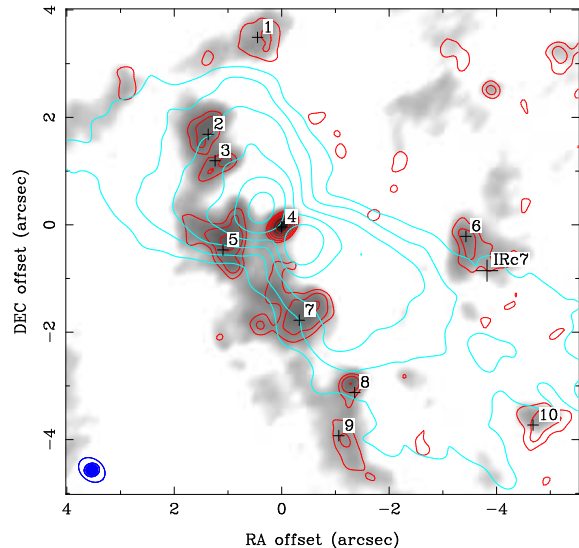


FIG. 1.— Comparison of 349 GHz continuum imaged with ALMA (halftone) and the 229 GHz continuum (red contours) and 86 GHz SiO  $v=0$  outflow (blue contours) imaged with CARMA. The SiO emission is averaged over the velocity range  $-10$  to  $+20 \text{ km s}^{-1}$  (Plambeck et al. 2009). The halftone scale is logarithmic from 0.01 to  $1 \text{ Jy/beam}$  in order to show the low level emission that traces the boundaries of the SiO outflow. Continuum peaks at 229 and 349 GHz agree well. Compact sources identified by Hirota et al. (2015) are marked by crosses; infrared source IRc7 is associated with peak 6. The contour levels are  $1,2,4,8,16 \times$  the lowest levels, which are 0.01 and  $0.08 \text{ Jy/beam}$  at 229 and 86 GHz, respectively.

associated with the Orion Hot Core. Spectral features which are *relatively* clear of confusing structure from other spectral lines are listed in Table 1. In Figure 2 we show emission in the  $\text{HC}_3\text{N}$  and HCN  $v=2$  transitions at 354.6975 and 356.2556 GHz in  $1 \text{ km s}^{-1}$  channels at velocities  $-10$ ,  $-3$ , and  $+12 \text{ km s}^{-1}$  superposed on the SiO  $v=0$  outflow.

#### 5. DISCUSSION

The images in Figures 1 and 2 provide important clues to the interaction of the outflow from SrcI with the ambient molecular cloud, and to heating of the Hot Core. Dust emission seems to trace the periphery of the SiO outflow. The Hot Core peaks lie along an arc  $\sim 1''$  east of SrcI where the SiO emission drops off steeply (note the log contours). Other ridges of dust emission are found along the NE, SE, and SW boundaries of the outflow. These observations suggest that the dust emission originates from the walls of a cavity formed by the outflow.

The  $\text{HC}_3\text{N}$  and HCN  $v=2$  molecular transitions shown in Figure 2 have upper state energy levels of 341 and 1067 K. Often the peak molecular emission is offset slightly from the dust clumps, suggesting that the molecular gas may be heated by the interaction of the outflow from SrcI with these clumps. Many SO and  $\text{SO}_2$  spectral lines with  $E_U$  from 180 to 1058 K also trace the boundaries of the outflow. The clearest example of this is shown in Figure 3 where we show the  $\text{SO}_2$  line at 342.7616 GHz averaged over LSR velocities  $-12$  to  $-7 \text{ km s}^{-1}$ , overlaid on the the SiO image.

Goddi et al. (2011a) imaged the Hot Core in  $\text{NH}_3$  transitions with upper energy levels 408 to 1456 K. Their observations show that the hottest gas lies in a ridge  $\sim 1''$

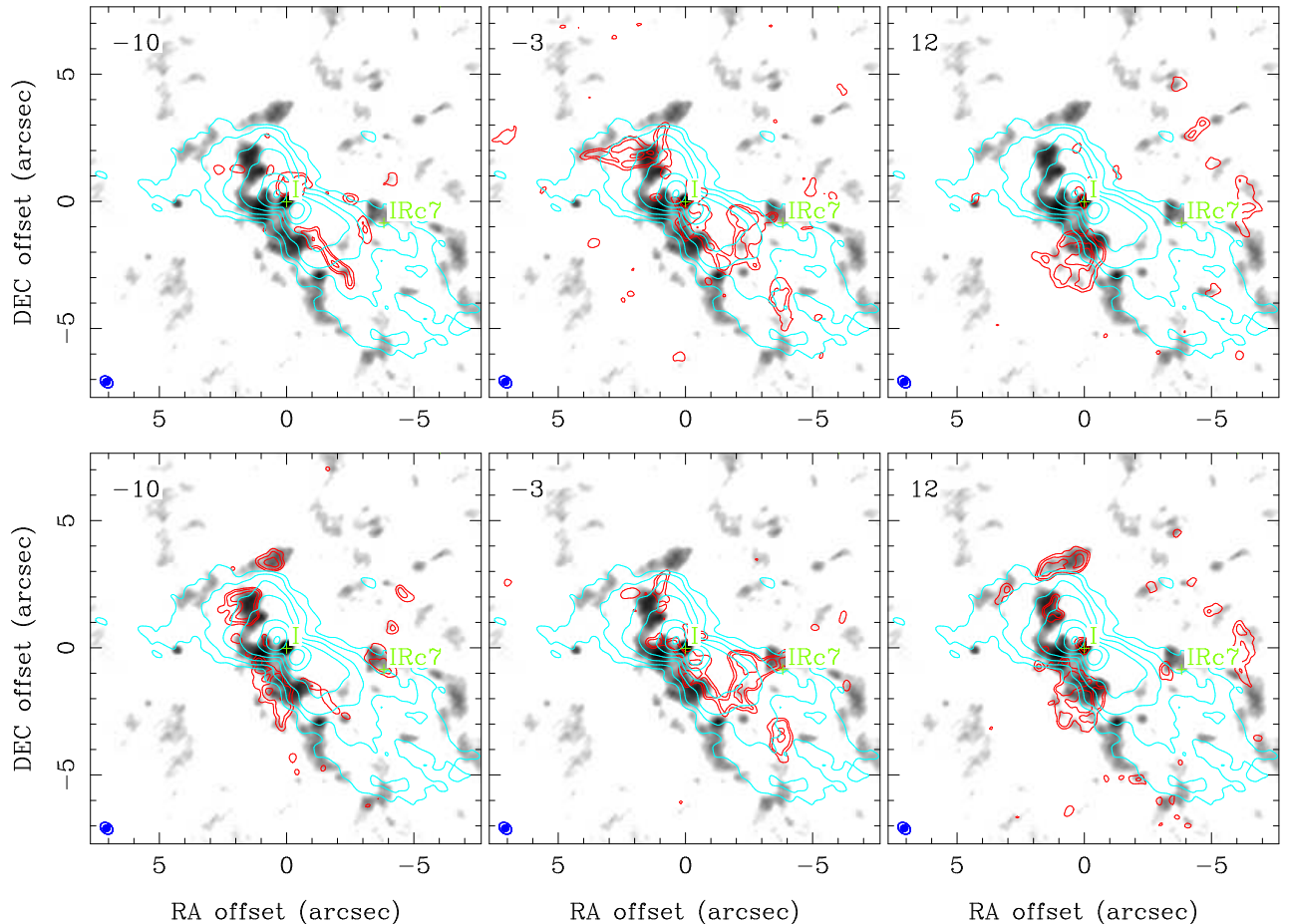


FIG. 2.— (top panels) Comparison of  $\text{HC}_3\text{N}$  emission with the 349 GHz dust continuum and the 86 GHz  $\text{SiO } v=0$  outflow from Orion SrcI. The  $\text{HC}_3\text{N}$  line at 354.6975 GHz is shown by red contours, with levels 0.1, 0.2, 0.4, 0.8 Jy/beam, in 1 km  $\text{s}^{-1}$  wide channels centered at LSR velocities of -10, -3, and +12 km  $\text{s}^{-1}$ . The 349 GHz dust continuum is indicated by the gray scale, logarithmic from 0.01 to 0.2 Jy/beam. The  $\text{SiO } v=0$  outflow is in blue contours, with levels 0.05, 0.1, 0.2, 0.4, ..., 3.2 Jy/beam. (bottom panels) Same, for the  $\text{HC}_3\text{N } v=2$  line at 356.2556 GHz, in red contours, again with levels 0.1, 0.2, 0.4, 0.8 Jy/beam. In all panels the FWHM synthesized beam for the Band 7 spectral lines is indicated by a filled blue ellipse, and for the  $\text{SiO } v=0$  outflow by the open ellipse.

to the SE of SrcI. They suggest that the Hot Core may be heated in C-type shocks driven by the outflow from SrcI, and by the proper motion of SrcI to the SE at  $\sim 12$  km  $\text{s}^{-1}$ . Peng et al. (2017) imaged the Hot Core in 64 transitions of  $\text{HC}_3\text{N}$  and  $^{13}\text{C}$  isotopologues. Their images of vibrationally excited  $\text{HC}_3\text{N}$  lines also show that the excitation peaks lie along the edge of the  $\text{SiO}$  outflow adjacent to the Hot Core. Both of these studies argue for an external source of heating for the Hot Core. Although some of the continuum peaks could contain embedded stars or protostars, spectral energy distributions for most of them suggest masses of only 0.02 to 0.2  $M_{\odot}$  (Hirota et al. 2015). Other observations in the radio and infrared find no evidence for excitation peaks within the Hot Core (Menten & Reid 1995; Greenhill et al. 2004). Together, these observations suggest that the outflow from SrcI may be heating the Hot Core and a shell of material tracing the boundaries of the  $\text{SiO}$  outflow.

### 5.1. Energetics

SrcI is the dominant source of luminosity in KL. At mm wavelengths SrcI appears to be an optically thick

dust disk with  $\sim 0.1''$  radius and temperature 500-700 K (Plambeck & Wright 2016; Hirota et al. 2016). A 100 AU diameter disk with temperature 700 K has a luminosity of  $\sim 10^4 L_{\odot}$ . The Hot Core is a clumpy structure with diameter  $\sim 10''$  and a dust temperature  $\sim 100 - 150$  K, optically thick in the far infrared. Modeling it as a spherical black body with  $\sim 1000$  AU radius, its luminosity is  $(0.4-2) \times 10^4 L_{\odot}$ . Thus, it appears that SrcI is capable of heating the Hot Core to its observed temperature.

Thermal excitation in 100-150 K gas does not, however, easily account for the high excitation ( $E_U > 500$  K) HCN and  $\text{SO}_2$  transitions in Figures 2 and 3, or the  $\text{HC}_3\text{N}$  and  $\text{NH}_3$  lines imaged by Peng et al. (2017) and Goddi et al. (2011a). Goddi et al. (2011a) suggest that the Hot Core is heated by shocks from the impact of the outflow from SrcI and its proper motion towards dense clumps in the Hot Core. The prominent abundance of SO and  $\text{SO}_2$  transitions also is indicative of shock chemistry. Models of C-type shocks with velocities 5-40 km  $\text{s}^{-1}$  can enhance SO and  $\text{SO}_2$  abundance by 2 orders of magnitude in the shock and extensively in the post shocked gas (Pineau des Forets et al. 1993).

We now consider whether the mechanical luminosity of

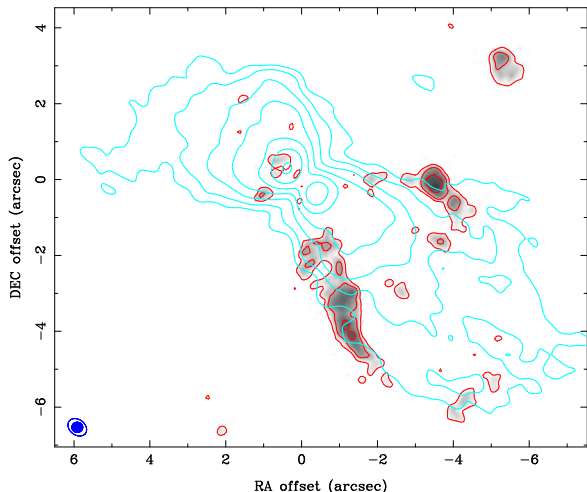


FIG. 3.— Molecular emission tracing the SiO outflow from SrcI.  $\text{SO}_2$  emission at 342.7616 GHz in the velocity range  $-12$  to  $-7$   $\text{km s}^{-1}$  is shown in red contour levels 0.02 0.04 0.08 0.16 Jy/beam and log grey scale from 0.02 to 0.2 Jy/beam. The SiO  $v=0$  outflow is shown in blue contours as in Figure 1. The synthesized beam FWHM for the Band 7 spectral lines is shown as the filled blue ellipse, and for the SiO  $v=0$  outflow as the open ellipse.

the SrcI outflow is sufficient to account for these shock-excited transitions. Wright et al. (1995) estimate the mass outflow from the  $J=2-1$ ,  $v=0$  SiO outflow  $\sim 10^{-5} M_{\odot} \text{ yr}^{-1}$ . A similar value ( $5 \times 10^{-6}$ ) was obtained for the SiO  $J=1-0$   $v=1$  masers by Greenhill et al. (2013). With a velocity  $\sim 18$   $\text{km s}^{-1}$ , the outflow luminosity is of order  $1 L_{\odot}$ . Assuming isotropic radiation and a velocity width of  $\sim 20$   $\text{km s}^{-1}$ , the luminosity of the high excitation HCN and  $\text{SO}_2$  lines in Figures 2 and 3 is  $\sim 1\text{-}10 \times 10^{-5} L_{\odot}$ . Hundreds, or perhaps thousands, of such lines are emitted by the Hot Core. Although it appears that the outflow does have sufficient mechanical luminosity to power these lines, a rather high conversion efficiency would be required.

### 5.2. Co-moving gas with SrcI

The explosive outflow associated with the dynamic interaction of BN and SrcI may also play a role in heating the Hot Core. Several studies suggest that the BN/KL outflow traced by fast moving CO and  $\text{H}_2$  bullets is associated with a wide angle outflow of  $5\text{-}10 M_{\odot}$  of gas with velocities  $\sim 20$   $\text{km s}^{-1}$  and may have a common origin in a dynamic interaction which ejected BN to the NW and SrcI to the SE  $\sim 500$  years ago (Gómez et al. 2008; Zapata et al. 2009; Goddi et al. 2011b; Bally et al. 2011, 2017). The kinetic energy of the BN/KL outflow is estimated as  $\sim 4 \times 10^{46}$  (Snell et al. 1984) to  $4 \times 10^{47}$  erg (Kwan & Scoville 1976). The  $\sim 20$   $\text{km s}^{-1}$  outflow and the fast moving bullets appear to be blocked by the Hot Core (Chernin & Wright 1996; Zapata et al. 2011).

The impact of this outflow on the Hot Core may also be responsible for shock heating of high excitation molecules (Zapata et al. 2011; Goddi et al. 2011a). Zapata et al. (2011) note that the high excitation lines  $\text{HC}_3\text{N}$   $37\text{-}36$   $v_7=1$  and  $\text{CH}_3\text{OH}$   $7_{4,3} - 6_{4,3}$   $v_t = 2$  appear to form a shell around the Hot Core peaks, as is also observed for  $\text{HC}_3\text{N}$  and HCN in our ALMA observations. It may

be possible to identify the origin of the molecular material: apparently oxygen-rich material ( $\text{SiO}$ ,  $\text{H}_2\text{O}$ ,  $\text{OH}$ ,  $\text{SO}$ ,  $\text{SO}_2$ ), from the SrcI outflow, and  $\text{NH}_3$ ,  $\text{HC}_3\text{N}$ , HCN,  $\text{CH}_3\text{CN}$ , etc. from the Hot Core.

If the motion of SrcI is accompanied by co-moving gas, this helps to explain why the SiO outflow from SrcI is not swept back by its motion though the ambient gas. Magnetic support has been invoked to explain the collimation of the SrcI outflow into a straight bipolar flow (e.g., Greenhill et al. 2013; Vaidya & Goddi 2013), and millimeter wavelength polarization observations (Tsuboi et al. 1996; Plambeck et al. 2003) suggest a polarization parallel to the SrcI outflow, but the field strength is as yet undetermined, and it is not clear if magnetic fields control the direction of the outflow, or vice versa.

Any original disk around SrcI was stripped off in the BN/SrcI encounter (Bally et al. 2017). Co-moving gas also helps re-formation of a disk around SrcI through Bondi-Hoyle, B-H, accretion. The B-H radius  $R_{BH} \sim GM/v^2$ . The accretion rate  $\dot{M}_{BH} = \pi\rho R^2 v$  so  $\dot{M} \sim 1/v^3$  and B-H accretion could re-form a disk around SrcI if the relative velocity of SrcI w.r.t. the ambient gas is only a few  $\text{km s}^{-1}$ . For example, with a relative velocity of  $2$   $\text{km s}^{-1}$  through an ambient density  $n(\text{H}_2) \sim 10^6 \text{ cm}^{-3}$ , SrcI could accrete a disk mass  $\sim 0.07 M_{\odot}$ , consistent with an estimated  $0.02 - 0.2 M_{\odot}$  for the dusty disk model in (Plambeck & Wright 2016).

### 5.3. Molecular Ring

Figure 4 shows a molecular ring,  $\sim 2''$  south of SrcI and centered at RA = 05:35:14.535 DEC = -05:22:32.7  $\pm 0.1''$  in  $\text{HC}_3\text{N}$  at 354.6975 GHz and HCN  $v=2$  at 354.4606 GHz in  $1$   $\text{km s}^{-1}$  channels at velocities from  $9$  to  $14$   $\text{km s}^{-1}$ . The ring presents an almost complete shell with a diameter  $\sim 2.6 \times 1.9''$  in position angle  $-30$  to  $-50$  deg. The shell width decreases from  $10$  to  $14$   $\text{km s}^{-1}$  with a velocity gradient across the minor axis in PA  $\sim 45$  deg. The ring can also be seen in the SO and  $\text{SO}_2$  lines listed in Table 1 with  $E_U$  from  $180$  to  $678$  K. It is not apparent in the lower excitation  $\text{SO}_2$  lines where the emission may be optically thick, or in the higher excitation lines with  $E_U > 800$  K. The high energy levels suggest shock excitation, perhaps from high velocity ejecta from the BN/SrcI explosion. A rotating, expanding shell model is possible. There is no evidence for the red-shifted cap of the ring at velocities  $> 14$   $\text{km s}^{-1}$ , but this could have been dispersed by shear motions of the outflow from SrcI. An expansion velocity  $\sim 2$   $\text{km s}^{-1}$  with a ring radius  $\sim 300$  AU gives a dynamical age  $\sim 700$  yr; a rotation velocity  $\sim 2$   $\text{km s}^{-1}$  gives an equilibrium mass  $\sim 0.2 M_{\odot}$ . If the ring resulted from an impact on a dust clump with ejecta from the BN/SrcI explosion  $\sim 500$  years ago then the ring has been decelerated by swept up material. C-type shocks with velocities as low as  $10$   $\text{km s}^{-1}$  can completely remove the grain mantles and produce gas kinetic temperatures to  $500$  K (Flower & Pineau des Forets 1994). Some of the compact features in the Hot Core identified by Hirota et al. (2015) might be ejecta from the BN/SrcI explosion. We did not detect any continuum emission at the center of the ring in any of the observations reported here. The dust source SMA1, Hirota source number 7, is at the edge of the ring as shown in Figure 4.

## 6. SUMMARY

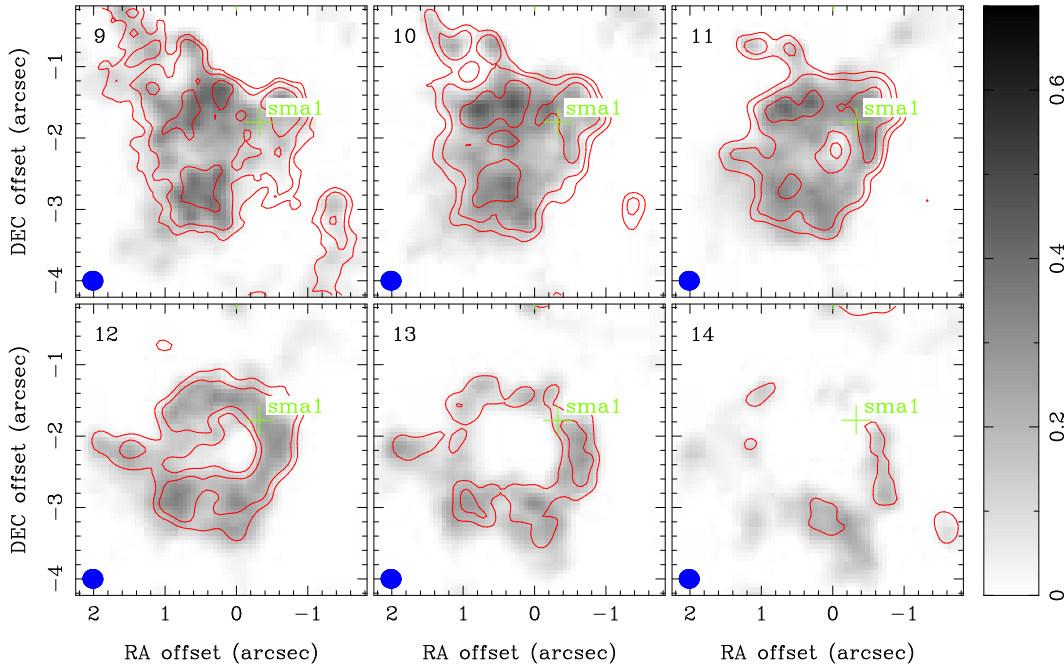


FIG. 4.— Molecular ring shown in  $\text{HC}_3\text{N}$  at 354.6975 GHz in grey scale, and  $\text{HCN } v=2$  at 354.4606 GHz in red contours in  $1 \text{ km s}^{-1}$  channels at velocities 9 to 14  $\text{km s}^{-1}$ . The grey scale is from 0 to 0.7  $\text{Jy/beam}$ . Band 7 continuum emission has been subtracted from the spectral lines. The synthesized beam FWHM for the Band 7 spectral lines is shown as the filled blue ellipse.

The Orion Hot Core was imaged with ALMA at 349 GHz with  $\sim 0''.2$  angular resolution. Our observations offer support for a model where the Hot Core is heated by shocks produced by the outflow from SrcI and from the BN/KL explosive event. A measurement of the proper motion of the most compact features in the Hot Core clumps w.r.t. SrcI, if technically feasible, could reveal whether the Hot Core itself is party to the expansion resulting from the BN/SrcI encounter.

We would like to thank an anonymous referee for helpful comments which have improved this paper. This paper makes use of the following ALMA data: ADS/JAO.ALMA#2012.1.00123.S. ALMA is a partnership of ESO (representing its member states), NSF

(USA) and NINS (Japan), together with NRC (Canada) and NSC and ASIAA (Taiwan), in cooperation with the Republic of Chile. The Joint ALMA Observatory is operated by ESO, AUI/NRAO and NAOJ.

The National Radio Astronomy Observatory is a facility of the National Science Foundation operated under cooperative agreement by Associated Universities, Inc.”

Support for CARMA construction was derived from the states of California, Illinois, and Maryland, the James S. McDonnell Foundation, the Gordon and Betty Moore Foundation, the Kenneth T. and Eileen L. Norris Foundation, the University of Chicago, the Associates of the California Institute of Technology, and the National Science Foundation.

*Facilities:* CARMA, ALMA.

#### REFERENCES

- Bally, J., Cunningham, N. J., Moeckel, N., et al. 2011, *ApJ*, 727, 113
- Bally, J., Ginsburg, A., Arce, H., et al. 2017, *ApJ*, 837, 60
- Chernin, L. M., & Wright, M. C. H. 1996, *ApJ*, 467, 676
- Flower, D. R., & Pineau des Forets, G. 1994, *MNRAS*, 268, 724
- Goddi, C., Greenhill, L. J., Humphreys, E. M. L., Chandler, C. J., & Matthews, L. D. 2011a, *ApJ*, 739, L13
- Goddi, C., Humphreys, E. M. L., Greenhill, L. J., Chandler, C. J., & Matthews, L. D. 2011b, *ApJ*, 728, 15
- Gómez, L., Rodríguez, L. F., Loinard, L., et al. 2008, *ApJ*, 685, 333
- Greenhill, L. J., Gezari, D. Y., Danchi, W. C., et al. 2004, *ApJ*, 605, L57
- Greenhill, L. J., Goddi, C., Chandler, C. J., Matthews, L. D., & Humphreys, E. M. L. 2013, *ApJ*, 770, L32
- Hirota, T., Kim, M. K., Kurono, Y., & Honma, M. 2015, *ApJ*, 801, 82
- Hirota, T., Machida, M. N., Matsushita, Y., et al. 2016, *ApJ*, 833, 238
- Kim, M. K., Hirota, T., Honma, M., et al. 2008, *PASJ*, 60, 991
- Kwan, J., & Scoville, N. 1976, *ApJ*, 210, L39
- Matthews, L. D., Greenhill, L. J., Goddi, C., et al. 2010, *ApJ*, 708, 80
- Menten, K. M., & Reid, M. J. 1995, *ApJ*, 445, L157
- Menten, K. M., Reid, M. J., Forbrich, J., & Brunthaler, A. 2007, *A&A*, 474, 515
- Peng, Y., Qin, S.-L., Schilke, P., et al. 2017, *ApJ*, 837, 49
- Pineau des Forets, G., Roueff, E., Schilke, P., & Flower, D. R. 1993, *MNRAS*, 262, 915
- Plambeck, R. L., & Wright, M. C. H. 2016, *ApJ*, 833, 219
- Plambeck, R. L., Wright, M. C. H., & Rao, R. 2003, *ApJ*, 594, 911
- Plambeck, R. L., Wright, M. C. H., Friedel, D. N., et al. 2009, *ApJ*, 704, L25
- Plambeck, R. L., Bolatto, A. D., Carpenter, J. M., et al. 2013, *ApJ*, 765, 40
- Snell, R. L., Scoville, N. Z., Sanders, D. B., & Erickson, N. R. 1984, *ApJ*, 284, 176
- Tsuboi, M., Ohta, E., Kasuga, T., Murata, Y., & Handa, T. 1996, *ApJ*, 461, L107
- Vaidya, B., & Goddi, C. 2013, *MNRAS*, 429, L50

Wright, M. C. H., Plambeck, R. L., Mundy, L. G., & Looney,  
L. W. 1995, ApJ, 455, L185

Zapata, L. A., Loinard, L., Schmid-Burgk, J., et al. 2011, ApJ,  
726, L12

Zapata, L. A., Schmid-Burgk, J., Ho, P. T. P., Rodríguez, L. F.,  
& Menten, K. M. 2009, ApJ, 704, L45